Elasticity of two-dimensional filaments with constant spontaneous curvature

Zicong Zhou*

Department of Physics and Graduate Institute of Life Sciences, Tamkang University, 151 Ying-chuan, Tamsui 25137, Taiwan, Republic of China

(Received 26 January 2007; revised manuscript received 16 July 2007; published 20 December 2007)

We study the mechanical property of a two-dimensional filament with constant spontaneous curvature and under uniaxial applied force. We derive the equation that governs the stable shape of the filament and obtain analytical solutions for the equation. We find that for a long filament with positive initial azimuth angle (the azimuth angle is the angle between x axis and the tangent of the filament) and under large stretching force, the azimuth angle is a two-valued function of the arclength, decreases first, and then increases with increasing arclength. Otherwise, the azimuth angle is a monotonic function of arclength. At finite temperature, we derive the differential equation that governs the partition function and find exact solution of the partition function for a filament free of force. We obtain closed-form expressions on the force-extension relation for a filament under low force and for a long filament under strong stretching force. Our results show that for a biopolymer with moderate length and not too small spontaneous curvature, the effect of the spontaneous curvature cannot be replaced by a simple renormalization of the persistence length in the wormlike chain model.

DOI: 10.1103/PhysRevE.76.061913 PACS number(s): 87.15.−v, 82.37.Rs, 36.20.Ey, 87.16.Ac

I. INTRODUCTION

The mechanical properties of semiflexible biopolymers have attracted considerable attention due to their importance in understanding many biological processes. Recent progresses in experimental techniques, such as laser or magnetic tweezers, atomic force microscopy, and other single molecule techniques, have provided powerful tools to manipulate and observe directly the mechanical response of a single biomolecule. In theoretical studies, a biopolymer is often modelled by a filament. In a first approximation, a filament can be viewed as an inextensible chain with a uniform bending rigidity but with a negligible cross section. This is called wormlike chain (WLC) model and has been used successfully to account for the entropic elasticity of double-stranded DNA (dsDNA) [1–4]. Owing to the central role that dsDNA plays in biology, recently there are many theoretical works on the WLC model, as well as its modifications and extensions [1–25] .

There is just one parameter, the bending rigidity, in the WLC model. In other words, WLC model is in essential a homogeneous model. However, biopolymers are in general sequence-dependent and so are heterogeneous. Several recent works have revealed that the sequence-disorder has remarkable effects on the conformational and mechanical properties of dsDNA [18–20,22,21,23]. Based on the WLC model, two effects of sequence-dependence have to be considered. First, structural inhomogeneity results in variations of the bending rigidity along the chain and can be described by the s-dependent persistence length [21], where s is the arclength. For long DNA chains without long-range correlation (LRC) in basepairs, this effect can be well accounted by a simple replacement of the uniform persistence length in the WLC model by a proper average of the s-dependent persistence length [21]. However, for loop formation in a short DNA chain, this effect is complex due to the lack of self-averaging: The looping probability of a typical filament segment is not a well-defined function of its length, not even to the first approximation [21]. The similar effect may also exist in other properties, such as elasticity. Second, the local structure of the dsDNA can be characterized by the sequence-dependent spontaneous curvature $c_0(s)$ [18–23]. For short dsDNA chains, special sequence orders may favor a macroscopic spontaneous curvature [32–35]. On the other hand, for long dsDNA chains, the effects of $c_0(s)$ are dependent on the degree of correlation in base pairs. Without correlation, or the correlation is short range, the effect is similar to that of the s-dependent persistence length and can be replaced by a renormalization of the persistence length in the WLC model [19–21,23]. However, with long-range correlation, such as dsDNA fragments extracted from intergenic regions in chromosome 8 (125789398-125791587) and 21 (37044232-37046437) of the human genome (NCBI build 35), the simple correction to the uniform persistence length is no longer appropriate because the dsDNA develops a macroscopic intrinsic curvature [23]. Moreover, it has been found that the mean spontaneous curvature, rather than the details of its distribution, determines the looping probability of a filament [22]. Therefore, to study the mechanical properties of the biopolymers with special sequence order or with LRC, a reasonable, and perhaps the simplest idea is to extend the WLC model so as to include a constant spontaneous curvature. Furthermore, a biopolymer in vivo is often subjected to confinement, such as a dsDNA in cell. Therefore, the property of biopolymers under confinement has attracted growing interest in the past decade [23,24,26–31]. Consequently, it is a significant topic to study the effect of a uniform spontaneous curvature on the elastic response for a confined, or two-dimensional, filament.

In this work, we examine the conformations and elasticity of a two-dimensional filament with constant spontaneous curvature and under uniaxial applied force. We obtain analytical solutions for the equation that governs the stable

*zzhou@mail.tku.edu.tw

shape of the filament and find that the form of these solutions are dependent on the direction of applied force and boundary conditions. At finite temperature, we derive the differential equation that governs the partition function, and find the exact solution for the partition function for a filament free of force. This partition function is further used to find the closed-form expression for the end-to-end distance, and the force-extension relation for a filament under low force. We also find the force-extension relation for a long filament under strong stretching force.

This paper is organized as follows. In Sec. II we set up our model and derive the shape equation for a stable filament. Section III presents the solutions for the shape equation. In Sec. IV we investigate the effects of the spontaneous curvature on the end-to-end distance and the elastic properties of the filament at finite temperature. A summary concludes the paper.

II. MODEL AND SHAPE EQUATION

Using s as variable, the configuration of a uniform filament with negligible cross section can be described by the tangent, $\mathbf{t}$, to the contour line of the filament. In two dimension, $\mathbf{t}=\{\cos\phi(s),\sin\phi(s)\}$, where the azimuth angle ϕ is the angle between x axis and $\mathbf{t}$. The locus of the filament can be found by

$$\mathbf{r}(s)=\{x(s),y(s)\}=\left\{\int_0^s \cos\phi(u)du,\int_0^s \sin\phi(u)du\right\}. \tag{1}$$

The energy of the filament with uniform spontaneous curvature $c_0(>0$ for convenience) and under a uniaxial applied force f_x (along x axis; $f_x<0$ for compression) can be written

$$E=\int_0^L \left[\frac{\kappa}{2}(\dot{\phi}-c_0)^2-f_x\cos\phi\right]ds, \tag{2}$$

where $\dot{X}\equiv dX/ds$, L is the total arclength of the filament and is a constant in the model so that the filament is inextensible, and κ is the bending rigidity.

When the thermal fluctuations are negligible, the static conformations of the filament are determined by the minimum of E. Extremizing E, we obtain the equation that governs the shape of the filament

$$\kappa\ddot{\phi}-f_x\sin\phi=0. \tag{3}$$

In experiments, the initial azimuth angle ϕ_0 may be fixed. In this case, the boundary condition (BC) at $s=0$ is $\phi(0)=\phi_0$. The extremum in the energy requires that at the other end $(s=L)$

$$\dot{\phi}_L-c_0=0, \tag{4}$$

where $\phi_L=\phi(L)$. However, experiments on stretching biopolymers usually involves attaching the two ends of the molecule to beads, and it does not seem to be easy to prohibit the rotation of the beads. As a consequence, it may be difficult to fix ϕ_0. In extreme cases, the filament can rotate freely around the origin, and so similar to Eq. (4), the BC at $s=0$ becomes

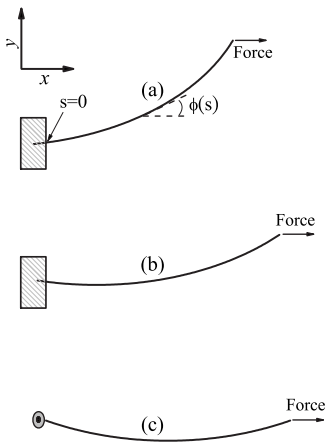

FIG. 1. Schematic picture of a filament under different boundary conditions. (a) ϕ_0 is fixed by grafting a small portion of filament to a substrate. $\phi_0=0.2$. (b) The same as (a) except for $\phi_0=-0.2$. (c) One end of the filament is attached to a bead, which is confined by a pivot. ϕ_0 is not fixed so the bead can rotate freely around the pivot. $c_0=0.1$ and $L=10$ for all three cases.

$$\dot{\phi}_0-c_0=0. \tag{5}$$

The pictorial representations of a filament under different BCs are shown in Fig. 1. In Figs. 1(a) and 1(b), ϕ_0 is fixed by grafting a small portion of filament to a substrate. For biopolymers, optical tweezer can be used to fix ϕ_0 [25]. In Fig. 1(c), the filament is attached to a bead and the center of the bead is confined by a pivot, but the bead can rotate freely around the pivot so ϕ_0 can be arbitrary. In experiments for biopolymers, magnetic tweezer can be used to maintain a free ϕ_0 [25]. It is clear that there is not symmetry with respect to x axis if $c_0\neq 0$. It has been reported that with or without constraint on the initial azimuth angle has considerable effects on the mechanical response of a filament [17,25]. In this work, we further find that, due to the break of symmetry with respect to y direction, the sign of ϕ_0 also has important effects on the mechanical response of a filament.

Defining the reduced force $F_x\equiv 2f_x/\kappa$, from Eqs. (3) and (4) we can find that

$$\dot{\phi}^{\pm}(s)=\pm\sqrt{c_0^2+F_x(\cos\phi_L-\cos\phi)} \tag{6}$$

or

$$s(\phi^{\pm})=\pm\int_{\phi_0}^{\phi}\frac{dx}{\sqrt{c_0^2+F_x(\cos\phi_L-\cos x)}}, \tag{7}$$

in which ϕ_L is determined by

$$L=\pm\int_{\phi_0}^{\phi_L}\frac{dx}{\sqrt{c_0^2+F_x(\cos\phi_L-\cos x)}}. \tag{8}$$

Note that both $\phi^+(s)$ and $\phi^-(s)$ are monotonic functions of s, but $\dot{\phi}^-(s)<0$ so it cannot satisfy BC at $s=L$ since we assume $c_0>0$ for convenience.

The stable (or at least metastable) of a filament requires

$$\delta^2 E = \int_0^L [\kappa \delta\dot{\phi}^2 + f_x \cos\phi \delta\phi^2] ds > 0. \tag{9}$$

When $f_x > 0$, the force tends to straighten the filament so $\cos\phi$ tends to be positive. Consequently, in this case the solution given by Eqs. (7) and (8) is, at least, metastable.

III. STABLE CONFORMATIONS OF A FILAMENT UNDER EXTERNAL FORCE

A. Filament with vanishing spontaneous curvature

In this case, if $\phi_0 = 0$ or ϕ_0 is free, the shape is simply a straight line. Moreover, from symmetry we need to consider only the case with $\phi_0 > 0$. It is well known that the end of the filament at $s = L$ tends to align along the direction of the applied force. Therefore, if $F_x > 0$, we should have $\phi_L < \phi_0$; since the direction of applied force is along $\phi = 0$, it follows that the solution of the shape equation is given by ϕ^- or

$$s = -\int_{\phi_0}^{\phi} \frac{dx}{\sqrt{F_x(\cos\phi_L - \cos x)}}, \tag{10}$$

$$L = -\int_{\phi_0}^{\phi_L} \frac{dx}{\sqrt{F_x(\cos\phi_L - \cos x)}}. \tag{11}$$

Let

$$k_0 \equiv \cos(\phi_L/2), \tag{12}$$

$$\cos(\phi/2) = k_0 \sin\theta, \tag{13}$$

we obtain (see Appendix A)

$$\phi(s) = 2 \arccos\left[k_0 \,\mathrm{sn}\left(\sqrt{\frac{F_x}{2}} s + F(\theta_0^0 | k_0) | k_0 \right) \right], \tag{14}$$

where $\mathrm{sn}(x|k)$ is the Jacobi elliptic function, $F(\theta|k)$ is the elliptic integral of the first kind, and $\theta_0^0 = \arcsin[\cos(\phi_0/2)/k_0]$.

In contrast, if $F_x < 0$, we should have $\phi_L > \phi_0$, since the direction of force is along $\phi = \pi$, and so the solution is given by ϕ^+. Let $k_0' = \sin(\phi_L/2)$, we find (see Appendix A)

$$\phi(s) = 2 \arcsin\left[k_0' \,\mathrm{sn}\left(\sqrt{\frac{-F_x}{2}} s + F(\beta_0 | k_0') | k_0' \right) \right], \tag{15}$$

where $\beta_0 = \arcsin[\sin(\phi_0/2)/k_0']$.

We should address that one must take care in using Eq. (13) [as well as $\cos(\phi/2) = k \sin\theta$ used in the following subsections] to transform the solution into $\mathrm{sn}(x|k)$ because the signs of ϕ and θ may be length-dependent. But note that the treatment in this section is in fact inappropriate for a very long filament since, in this case, the thermal fluctuation becomes significant; we do not consider a very long filament in this section. As a consequence, we do not consider a looped filament, and limit $-\pi < \phi < \pi$. Similarly, the case with a large $|\phi_0|$ is also not considered. Under these constraints, the solutions in the form of $\mathrm{sn}(x|k)$ should be still valid.

B. Filament with free initial azimuth angle

If we do not fix ϕ_0, then to satisfy BCs at both ends [Eqs. (4) and (5)], we need to take + in the right-hand side of Eq. (6), and so $\phi(s)$ increases monotonically with increasing s. Moreover, two BCs also lead to

$$\dot{\phi}(s) = \sqrt{c_0^2 + F_x(\cos\phi_L - \cos\phi)} = \sqrt{c_0^2 + F_x(\cos\phi_0 - \cos\phi)}. \tag{16}$$

It follows that $\cos\phi_L = \cos\phi_0$ or $\phi_L = -\phi_0 \geq 0$ since $\phi_L \geq \phi(s) \geq \phi_0$. It in turn indicates that a filament prefers to have a negative ϕ_0 if $c_0 > 0$, and so to fix the filament with a positive ϕ_0 requires extra force. Therefore, the solution for the shape equation becomes

$$s(\phi) = \int_{\phi_0}^{\phi} \frac{dx}{\sqrt{c_0^2 + F_x(\cos\phi_L - \cos x)}}, \tag{17}$$

$$L = 2\int_0^{\phi_L} \frac{dx}{\sqrt{c_0^2 + F_x(\cos\phi_L - \cos x)}}. \tag{18}$$

To get real values for the above integrations, it requires $c_0^2/F_x + \cos\phi_L - 1 \geq 0$. Therefore, let

$$k^2 \equiv \frac{1}{2}\left(1 + \frac{c_0^2}{F_x} + \cos\phi_L\right), \tag{19}$$

we have $k \geq 1$. In this case, the solution can be transformed into (see Appendix A)

$$\phi(s) = \pi - 2\,\mathrm{am}\left(-\sqrt{\frac{F_x}{2}} k s + F(\alpha_0 | k_1) | k_1 \right), \tag{20}$$

where $\mathrm{am}(x|k)$ is the Jacobi amplitude function, $\alpha_0 = \pi/2 - \phi_0/2$, and $k_1 = 1/k$. We can also show that (see Appendix A) this solution is symmetric with respect to the interchange of s and $L - s$. Moreover, in this case we should have $\phi(L/2) = 0$, $y(L) = y(0) = 0$, and the conformation is symmetric about $x = x(L/2)$. Furthermore, we do not consider the case with $F_x < 0$ since, in this case, we can rotate the coordinate system by 180° (but keep the force intact), thereby making it become the case with stretching force.

C. Filament with fixed initial azimuth angle and $\phi_0 > 0$

On the other hand, fixing ϕ_0 leads to quite different results. From Eq. (6), $\dot{\phi}^-(s) = -\sqrt{c_0^2 + F_x(\cos\phi_L - \cos\phi)} \leq 0$ so $\phi^-(s)$ fails to satisfy BC at $s = L$ [Eq. (4)] since $c_0 > 0$. Therefore, at first glance, the solution would be given by $\phi^+(s)$ alone. This argument is correct when $F_x < 0$. If $F_x > 0$, the argument is also correct when L is very short, or F_x is very small. In these cases, the shape of the filament is determined by

$$s = \int_{\phi_0}^{\phi} \frac{dx}{\sqrt{c_0^2 + F_x(\cos\phi_L - \cos x)}}, \tag{21}$$

$$L = \int_{\phi_0}^{\phi_L} \frac{dx}{\sqrt{c_0^2 + F_x(\cos\phi_L - \cos x)}}. \tag{22}$$

If $F_x > 0$, we can follow the same routine as for Eqs. (14) and (20) to find

$$\phi(s) = \begin{cases} 2\arccos\left[k\,\mathrm{sn}\left(-\sqrt{\frac{F_x}{2}}s + F(\theta_0|k)|k\right)\right], & k < 1, \\ \pi - 2\,\mathrm{am}\left(-\sqrt{\frac{F_x}{2}}ks + F(\alpha_0|k_1)|k_1\right), & k > 1, \end{cases} \tag{23}$$

where $\theta_0 = \arcsin[k_1 \cos(\phi_0/2)]$.

In contrast, if $F_x < 0$, let $k'^2 \equiv 2/(1 - c_0^2/F_x - \cos\phi_L)$, in a way similar to that for Eq. (15), we obtain

$$\phi(s) = \begin{cases} 2\,\mathrm{am}\left(\sqrt{\frac{-F_x}{2}}k_1' s + F(\phi_0/2|k')|k'\right), & k' < 1, \\ 2\arcsin\left[k_1'\,\mathrm{sn}\left(\sqrt{\frac{-F_x}{2}}s + F(\gamma_0|k_1')|k_1'\right)\right], & k' > 1, \end{cases} \tag{24}$$

where $k_1' = 1/k'$, and $\gamma_0 = \arcsin[k' \sin(\phi_0/2)]$.

However, for a long filament with $\phi_0 > 0$ and under strong stretching force, Eqs. (21)–(23) are incorrect. We can see this point by noting that, if $\phi(s) = \phi^+(s)$, then $\phi_L \geq \phi(s) \geq \phi_0$ so $\cos\phi_L - \cos\phi < 0$, and ϕ_L would be determined by

$$L = \int_{\phi_0}^{\phi_L} \frac{dx}{\sqrt{c_0^2 + F_x(\cos\phi_L - \cos x)}}. \tag{25}$$

To get a real L it requires $c_0^2 + F_x(\cos\phi_L - \cos x) \geq c_0^2 + F_x(\cos\phi_L - \cos\phi_0) \geq 0$. Therefore, we have $\cos\phi_L \geq \cos\phi_0 - c_0^2/F_x$, and so ϕ_L is bounded by $\arccos(\cos\phi_0 - c_0^2/F_x) \geq \phi_L > \phi_0$. Consequently, as shown in Appendix A, with $\phi_0 > 0$ and bounded ϕ_L, the right-hand side in Eq. (25) is also bounded for given c_0, F_x, and ϕ_0. Furthermore, note that c_0, F_x, and ϕ_0 are independent on L; such a bound in the right-hand side in Eq. (25) reveals that L cannot be arbitrarily large, it in turn tells us that Eqs. (21)–(23) are incorrect in this case.

Therefore, for large L there exists a special force F_x^s. When $F_x > F_x^s$, the solution is no longer $\phi^+(s)$ alone, but must be a combination of ϕ^+ and ϕ^-. We find that the larger the ϕ_0 or L, or the smaller the c_0, the smaller the F_x^s. As a consequence, there exists a special length l. When $s < l$, the solution is given by ϕ^-; however, when $s > l$, the solution is given by ϕ^+. In other words, for $F_x < F_x^s$, the solution is given by Eq. (23). But for $F_x > F_x^s$, the solution must be written as a piecewise function

$$s = \begin{cases} -\int_{\phi_0}^{\phi} \frac{dx}{\sqrt{c_0^2 + F_x(\cos\phi_L - \cos x)}}, & s < l, \\ l + \int_{\phi_l}^{\phi} \frac{dx}{\sqrt{c_0^2 + F_x(\cos\phi_L - \cos x)}}, & s > l. \end{cases} \tag{26}$$

This is also the unique case that $\phi(s)$ is a two-valued function of s, decreases first, down to the minimum value ϕ_l, and then increases with increasing s.

The continuity of $\dot{\phi}$ at l leads to $\dot{\phi}_l^+ = \sqrt{c_0^2 + F_x(\cos\phi_L - \cos\phi_l)} = \dot{\phi}_l^- = -\sqrt{c_0^2 + F_x(\cos\phi_L - \cos\phi_l)}$, or

$$c_0^2 + F_x(\cos\phi_L - \cos\phi_l) = 0 = \dot{\phi}_l. \tag{27}$$

From Eq. (6), we can show that $\ddot{\phi}(s)$ is also continuous at l. As a consequence, ϕ_L and $\phi_l (< \phi_0)$ are determined by

$$\phi_l = \arccos(c_0^2/F_x + \cos\phi_L), \tag{28}$$

$$L = -\int_{\phi_0}^{\phi_l} \frac{dx}{\sqrt{c_0^2 + F_x(\cos\phi_L - \cos x)}} + \int_{\phi_l}^{\phi_L} \frac{dx}{\sqrt{c_0^2 + F_x(\cos\phi_L - \cos x)}}. \tag{29}$$

There is not solution for Eq. (28) at low F_x due to $c_0^2/F_x + \cos\phi_L > 1$ and it is a consequence of that $l = 0$ when $F_x \leq F_x^s$. Moreover, our numerical calculations reveal that ϕ_l is always positive and quite close to zero. This can be understood by noting that if $\phi_l \sim 0$, then from Eq. (28) we obtain $c_0^2 + F_x(\cos\phi_L - \cos x) \sim F_x(1 - \cos x)$ and so L can be arbitrarily large, as shown in Appendix A 2.

Again, Eq. (26) can be expressed in terms of Jacobi elliptic function and elliptic integral. Since $\phi_l > 0$, we also have $\phi(s) \geq \phi_l > 0$, and if $k < 1$ the solution can be written as

$$\phi = \begin{cases} 2\arccos\left[k\,\mathrm{sn}\left(\sqrt{\frac{F_x}{2}}s + F(\theta_0|k)|k\right)\right], & s < l, \\ 2\arccos\left[k\,\mathrm{sn}\left(-\sqrt{\frac{F_x}{2}}(s-l) + F(\theta_l|k)|k\right)\right], & s > l, \end{cases} \tag{30}$$

where θ_l is determined by $\cos(\phi_l/2) = k \sin\theta_l$. In contrast, if $k > 1$, it would be better to use

$$\phi = \begin{cases} \pi - 2\,\mathrm{am}\left(\sqrt{\frac{F_x}{2}}ks + F(\alpha_0|k_1)|k_1\right), & s < l, \\ \pi - 2\,\mathrm{am}\left(-\sqrt{\frac{F_x}{2}}k(s-l) + F(\alpha_l|k_1)|k_1\right), & s > l, \end{cases} \tag{31}$$

where $\alpha_l = \pi/2 - \phi_l/2$.

It is a little surprise that our numerical calculations suggest that no matter how large the F_x may be, we always have $\phi_L > \phi_0$ if $\phi_0 > 0$, instead of $\phi_L \approx 0$ as common sense would

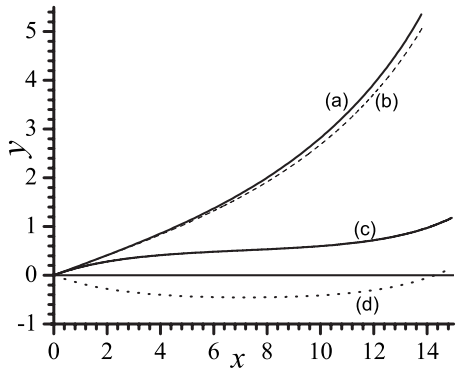

FIG. 2. Typical shapes of a two-dimensional filament under stretching. The parameters are $c_0=0.1$, $L=15$, and (a) (solid) $\phi_0=0.2$, $F_x=0.0373$; (b) (dash) $\phi_0=0.2$, $F_x=0.04$; (c) (solid) $\phi_0=0.2$, $F_x=0.3$; (d) (dot) $\phi_0=-0.2$, $F_x=0.3$. The unit of length and F_x are the same as $1/c_0$ and c_0^2, respectively.

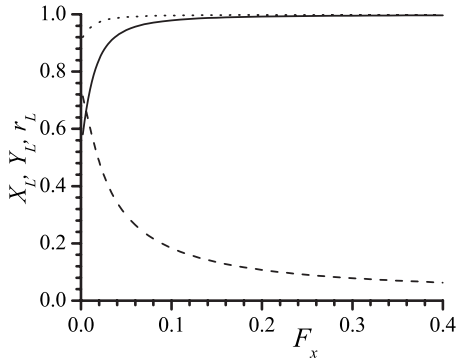

FIG. 3. Relative extension $X_L \equiv x(L)/L$ (solid), $Y_L \equiv y(L)/L$ (dash), and end-to-end distance (dot) $r_L \equiv \sqrt{X_L^2+Y_L^2}/L$ vs reduced force for a filament under stretching. The parameters are $c_0=0.1$, $\phi_0=0.2$, and $L=15$. The unit of length and F_x are the same as $1/c_0$ and c_0^2, respectively.

suggest. It should reflect the fact that under strong force, in fact it is impossible to fix ϕ_0. $\phi_L \approx 0$ under large F_x can be achieved when $\phi_0<0$.

Note that there is no such a finite l if $c_0=0$ no matter what the force. This is because, in this case, under stretching force ϕ_L can be close to 0 arbitrarily, and so from Eq. (8) L can be arbitrarily large. Therefore, the solution is given by ϕ^- solely.

From Eqs. (17)–(31), we can see that the expressions are different for the different BCs or the direction of force. The representations in terms of $F(x|k)$, $\mathrm{am}(x|k)$, and $\mathrm{sn}(x|k)$ allow numerical calculation by mathematical softwares like Mathematica [38] in most cases. However, when $F_x \approx F_c^c$, special care should be taken in using Eqs. (30) and (31) to calculate l because it may yield complex values, or have no solution at all, due to numerical error. This problem may result from the fact that at l, the integrand in Eq. (29) is singular [also see Eq. (27)] though the integration is convergent, therefore, evaluation of the inverse function at l numerically is uneasy, especially for our nontrivial algebraic functions, in which k is also dependent on ϕ_L and ϕ_l. In this case, using Eqs. (28) and (29) directly may be more reliable and simple.

Figures 2 and 3 shows some typical results. In both figures, $c_0=0.1$ and $L=15$. When $\phi_0=0.2$, we find that $F_x^s \approx 0.0373$. Figure 2 shows that the shapes with $\phi>0$ and $\phi<0$ are considerably different. From Fig. 3, we can find that x_L (y_L) increases (decreases) rapidly with increasing force when force is small, but changes very slowly under high force, and the increasing rate of x_L is faster than the decreasing rate of y_L at low force.

D. Filament with fixed initial azimuth angle and $\phi_0<0$

When $\phi_0<0$, the solution is simply given by ϕ^+. If $F_x>0$ and $k<1$, it can be written as

$$\phi(s)=\begin{cases} -2\arccos\left[k\,\mathrm{sn}\left(\sqrt{\frac{F_x}{2}}s+F(\theta_0|k)|k\right)\right], & \phi<0, \\ 2\arccos\left[k\,\mathrm{sn}\left(-\sqrt{\frac{F_x}{2}}s-F(\theta_0|k)+2F(\theta_1|k)|k\right)\right], & \phi>0, \end{cases} \tag{32}$$

where $\theta_1=\arcsin(1/k)$. In contrast, if $F_x>0$ and $k>1$, the solution is given by Eq. (20) again.

Unlike the case with $\phi_0>0$, now the solution does not need to be a piecewise function as in Eq. (26). This is because in this case k can be close to 1 and ϕ can be close to 0, so L is unbounded as shown in Appendix A 2. However, though mathematically it is undoubted, the underlying physics of such a ϕ_0 dependence is not very clear. Intuitionally, it is a consequence of that the existence of a constant spontaneous curvature leads to break of the symmetry with respect to y direction. Physically, it may be due to that the assumption of the inextensible total arclength in the model is unpractical for a long filament under strong force, but may be, more likely due to that, under strong force there is, in fact, no way to fix ϕ_0 since a filament tends to have a negative ϕ_0. Moreover, such a behavior may also arise from the assump-

tion of the constant curvature, so it may be unpractical for biopolymers, since few biopolymers have constant finite curvature throughout their length.

When $F_x<0$, the expression is the same as Eq. (24).

IV. ELASTICITY OF THE FILAMENT AT FINITE TEMPERATURE

A. Equation for the partition function

Up to now, the entropic effect has not been considered since the shape equation is obtained by extremizing energy. In principle, such a treatment is correct only at zero temperature. In practice, it is also a reasonable approximation when the thermal vibrations of the filament around its static conformation are negligible, such as at very low temperature or when the persistence length is comparable to the total length of the filament and at low to moderate temperature. Especially, it is usually valid for a macroscopic filament at room temperature. However, it is not appropriate for a long biopolymer at finite temperature because the temperature may induce strong conformation fluctuation and as a consequence the conformation of the filament can be far from the static one. Therefore, at finite temperature, it is, in general, necessary to perform conformational average. In this case, the partition function of the filament is the sum of Boltzmann weights for all possible conformations, and so is a path integral [24,36]

$$\mathcal{Z}(\phi_L,L;\phi_0,0)=\int \mathcal{D}[\phi(s)]e^{-\beta E}, \tag{33}$$

where $\beta\equiv 1/(k_BT)$, T is the temperature, and k_B is the Boltzmann constant. From (2) and (33), we can calculate the average end-to-end extension in x direction, $\langle x_L\rangle$, from

$$\langle x_L\rangle \equiv \left\langle \int_0^L \cos\phi(s)ds \right\rangle = \frac{\partial \ln \mathcal{Z}}{\partial f}, \tag{34}$$

where $f\equiv f_x\beta$. $\langle x_L\rangle$ is the conformational average of the end-to-end vector $\mathbf{R}=\int_0^L \mathbf{t}\,ds$ projected in the direction of the applied force.

From the standard connection between the path integral and the Schrödinger equation, we can find that $\mathcal{Z}(\phi,s;\phi_0,s_0)$ satisfies the following partial differential equation [14,36]

$$\frac{\partial \mathcal{Z}}{\partial s}=\left(\frac{1}{2l_p}\frac{\partial^2}{\partial\phi^2}-c_0\frac{\partial}{\partial\phi}+f\cos\phi\right)\mathcal{Z}, \tag{35}$$

where $l_p\equiv\kappa\beta$ is the bare persistence length. $\mathcal{Z}(\phi,s;\phi_0,s_0)$ must be a periodic function of ϕ since there is no way to distinguish ϕ and $\phi+2\pi$.

If we fix ϕ_0, the BC for $\mathcal{Z}(\phi,s;\phi_0,s_0)$ becomes

$$\mathcal{Z}(\phi,s_0;\phi_0,s_0)=\delta(\phi-\phi_0). \tag{36}$$

But we should note here that, to fix ϕ_0 may be difficult, especially for a microscopic object. Therefore, proper average over ϕ_0 is, in general, necessary.

We can separate variables by assuming $\mathcal{Z}(\phi,s;\phi_0,s_0)=\psi(\phi,\phi_0)e^{-g(s-s_0)}$. $\psi(\phi,\phi_0)$ is also a periodic function of ϕ since $\mathcal{Z}$ is. It follows that

$$\left(\frac{1}{2l_p}\frac{d^2}{d\phi^2}-c_0\frac{d}{d\phi}+f\cos\phi\right)\psi=-g\psi. \tag{37}$$

Equation (37) is in the form of the Mathieu differential equation with damping. Let

$$\psi(\phi,\phi_0)=e^{c_0l_p\phi}G(\phi,\phi_0), \tag{38}$$

Eq. (37) is transformed into

$$\frac{d^2G}{d\phi^2}+(2gl_p-c_0^2l_p^2+2fl_p\cos\phi)G=0. \tag{39}$$

Equation (39) can be transformed further into the well known Mathieu differential equation [37]. The Mathieu equation always has a periodic solution and an aperiodic solution [37]. However, from Eq. (38), we know that $G(\phi,\phi_0)$ cannot be a periodic function of ϕ if $c_0\neq 0$ due to ψ is already a periodic function of ϕ and $l_p>0$. Since G deserves the aperiodic solution but the general properties of the aperiodic solution do not seem to be transparent, we will not discuss the general solution of Eq. (39) in this work. Instead, the partition function at $f=0$ and the exact force-extension relations at low and high force limits are presented here.

B. Average end-to-end distance for the filament free of external force

When $f=0$, Eq. (37) becomes

$$\left(\frac{1}{2l_p}\frac{d^2}{d\phi^2}-c_0\frac{d}{d\phi}\right)\psi=-g\psi. \tag{40}$$

The periodic boundary condition requires that $\psi(\phi,\phi_0)=Ae^{n\phi i}$ with n being an integer. Therefore,

$$g_n^0=\frac{n^2}{2l_p}+c_0ni \tag{41}$$

and

$$\mathcal{Z}=\sum_{n=-\infty}^{\infty}A_ne^{-g_n^0(s-s_0)+in\phi}. \tag{42}$$

From BC [Eq. (36)], we can find that $A_n=(1/2\pi)e^{-in\phi_0}$, as well as

$$\mathcal{Z}=\frac{1}{2\pi}+\frac{1}{\pi}\sum_{n=1}^{\infty}e^{-(n^2/2l_p)(s-s_0)}\cos[n(\phi-\phi_0-c_0(s-s_0))]. \tag{43}$$

The average end-to-end distance, $R^2\equiv\langle|\mathbf{r}_L-\mathbf{r}_0|^2\rangle$, is

$$R^2 = \left\langle \int_0^L ds \int_0^L ds' \mathbf{t}(s) \cdot \mathbf{t}'(s') \right\rangle$$
$$= \int_0^L ds \int_0^L ds' \int_0^{2\pi} d\phi \int_0^{2\pi} d\phi' Z(\phi, s; \phi', s') \mathbf{t}(s) \cdot \mathbf{t}'(s') Z(\phi', s'; \phi_0, s_0)$$
$$= 2 \int_0^L ds \int_0^s ds' e^{-(s-s')/2l_p} \cos[c_0(s-s')]$$
$$= \frac{4l_p}{(1+4l_p^2 c_0^2)^2} \{L - 2l_p + 4l_p^2 c_0^2 L + 8l_p^3 c_0^2 + [2l_p \cos(c_0 L) - 8l_p^3 c_0^2 \cos(c_0 L) - 8l_p^2 c_0 \sin(c_0 L)] e^{-L/2l_p}\}, \quad (44)$$

where we have used $\mathbf{t}(s) \cdot \mathbf{t}'(s') = \cos(\phi - \phi')$. Note that c_0 does not appear in the exponential term. With fixed bending rigidity κ, when $T \to 0$ we obtain $R^2 = 2[1 - \cos(c_0 L)]/c_0^2$, as it should be for the distance between two ends of an arc with radius of $1/c_0$. In contrast, when $T \to \infty$, we find that $R^2 = 0$. ϕ_0 does not appear in Eq. (44) so R^2 is independent on BC. In a similar way, we can also find $\langle x_L \rangle$ and $\langle x_L^2 \rangle$, as presented in Appendix B.

Equation (44) is valid for arbitrary T, L, c_0, and l_p. When $c_0 = 0$, Eq. (44) become

$$R_{wlc}^2 = 4l_p L \left[1 - \frac{2l_p}{L} \left(1 - e^{-L/2l_p} \right) \right], \quad (45)$$

it is exactly the same as the well known result for WLC model [23] (note that there is a difference of factor 2 between definitions of l_p in present work and Ref. [23]).

Furthermore, for a very long filament ($L \gg l_p$), we find

$$R^2 \approx \frac{4l_p L}{1 + 4l_p^2 c_0^2}. \quad (46)$$

Defining the effective persistence length l_p^{eff} for arbitrary L as

$$l_p^{\text{eff}} \equiv \frac{R^2}{4L}, \quad (47)$$

from Eq. (46) we find that for a very long filament we can recover result on R^2 in WLC model with a simple replacement of the bare persistence length l_p by an effective persistence length $l_p^{\text{eff}\,1}$ in the form of

$$\frac{1}{l_p^{\text{eff}\,1}} = \frac{1}{l_p} + \frac{1}{l_p^c}, \quad (48)$$

where $l_p^c = 1/4l_p c_0^2$. It is in the same form as $1/l_p^{\text{eff}\,2} = 1/l_p + 1/l_p^s$ [18,19,21], but different from $l_p^{\text{eff}\,3} = l_p(1 - 1/2\sqrt{l_p/l_p^s})$ [20], where l_p^s is the "static" persistence length resulted from the sequence disorder of base pairs. From Eq. (48) we also know that the finite c_0 tends to reduce the effective persistence length, similar to the effect of the sequence-dependence nature [18–21].

However, if L is not very long, such a simple replacement becomes poor, or even invalid, since other terms in Eq. (44) will also make significant contributions to R^2. The larger the c_0, the larger the discrepancy will be. At $c_0 = 0.2/l_p$, the discrepancy is less than 5%, so the replacement is still reasonable. But at $c_0 = 0.7/l_p$, the discrepancy can be over 30% so the replacement becomes very poor. From Fig. 4 we can see that the obvious discrepancy can last up to about $L = 20l_p$, which is rather long in experiments. For instance, $l_p \approx 50$ nm for dsDNA without LRC, so $20l_p$ corresponds to approximately 3000 basepairs. Moreover, from Eq. (45) we can know that $R_{wlc}^2/4L$ is a monotonic function of L. Our calculations show that if $c_0 l_p < 0.48$, l_p^{eff} is still a monotonic function of L. However, if $c_0 l_p > 0.48$, l_p^{eff} is no longer a monotonic function of L but may have multiple maxima, as we can see from curves (d), (e), and (f) in Fig. 5. The larger the c_0, the more maxima it will have. These results suggest that a constant c_0 has considerable impact on the property of a filament. These results are also consistent with the conclusion that for a DNA with LRC, the effects of the sequence disorder cannot be incorporated into a simple correction to the persistence length [23]. Furthermore, the existence of maxima is also consistent with experimental observations and computer simulations [23] (especially the Fig. 3 in Ref. [23]), and therefore strongly supports that the present model is reasonable in describing the elasticity of biopolymers with LRC.

The relationship between L_m, the length corresponds to the first maximum in l_p^{eff}, and $1/c_0$ is shown as filled circles

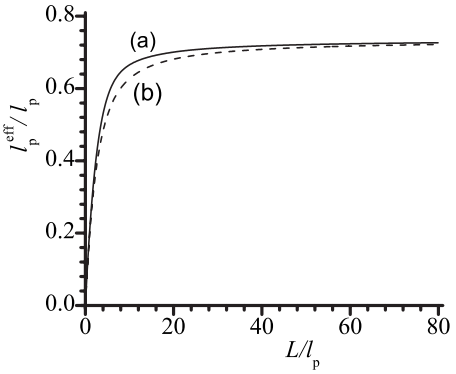

FIG. 4. Reduced effective persistence length, l_p^{eff}/l_p, vs reduced total arclength L/l_p for (a) present model [Eq. (44)], (b) WLC model [Eq. (45)], with a replacement of l_p by $l_p^{\text{eff}\,1}$ [Eq. (48)]. $c_0 l_p = 0.3$ in figure.

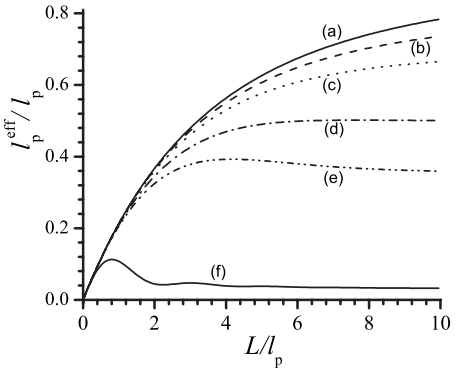

FIG. 5. l_p^{eff}/l_p vs L/l_p for a filament. The parameters are (a) $c_0 l_p=0.1$, (b) $c_0 l_p=0.2$, (c) $c_0 l_p=0.3$, (d) $c_0 l_p=0.5$, (e) $c_0 l_p=0.7$, and (f) $c_0 l_p=3$.

in Fig. 6. For comparison, in Fig. 6 we also plot the straight line given by $L_m'=\pi/c_0$ which corresponds to the arclength of a semicircle of a radius of $1/c_0$. From Fig. 6, we find that L_m decreases very fast and linearly at small c_0, but slowly at large c_0. $L_m \to 0$ when $c_0 \to \infty$ since $l_p^{\mathrm{eff}} \to 0$. We have tried several fitting functions, including different forms of polynomial functions and exponential functions, to fit the relationship between L_m and $1/c_0$, but none fit well for the whole regime. Moreover, we find that, in general, $L_m \neq \pi/c_0$. Instead, at small c_0, $L_m > \pi/c_0$; but at large c_0, from $dl_p^{\mathrm{eff}}/dL=0$ we find analytically that $L_m \approx 2.33/c_0 < \pi/c_0$. $L_m \approx \pi/c_0$ at $c_0 l_p \approx 0.6$. This result suggests that the entropic effect tends to reduce the looping probability for small c_0, but favors loop formation for large c_0. The conclusion, that the entropic effect favors looping for large c_0 is consistent with the three dimensional results [22]. But why the entropic effect tends to reduce the looping probability at small c_0 needs further investigation. Moreover, whether it is also valid in three dimensional cases or is only a special consequence of the confinement should be an intriguing issue for further research.

C. Elasticity of the filament under low force and strong force

From Eqs. (2), (33), and (34), it is straightforward to find that (with $x_L=\int_0^L \cos\phi\, ds$)

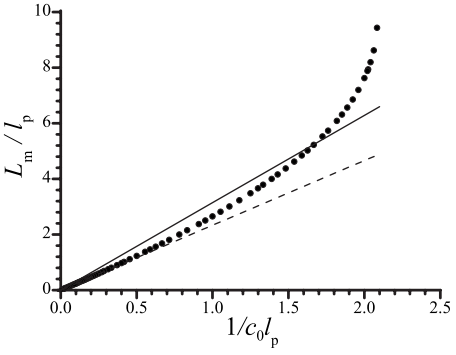

FIG. 6. Filled circles represent the relationship between L_m and $1/c_0$. The solid straight line and the dashed straight line have slopes π and 2.33, respectively.

$$\frac{\partial \langle x_L \rangle}{\partial f} = \langle x_L^2 \rangle - \langle x_L \rangle^2. \tag{49}$$

Therefore, under low force, the relation between f and extension ($\mathcal{X}$) can be found as

$$\mathcal{X} \equiv \langle x_L - \langle x_L \rangle_{f=0} \rangle = f[\langle x_L^2 \rangle_{f=0} - \langle x_L \rangle_{f=0}^2] = \frac{f l_p B}{(1+4c_0^2 l_p^2)^2 (9+4c_0^2 l_p^2)(1+c_0^2 l_p^2)}, \tag{50}$$

where B is presented in Appendix B. Note that B is dependent on ϕ_0. Equation (50) is valid for arbitrary L and T with fixed ϕ_0. When $c_0=0$ and L is very long, we obtain $\mathcal{X} \approx 2 f l_p L$, which is exactly the same as the existing result for WLC model [24,41].

If we cannot constrain ϕ_0, we need to average over all possible ϕ_0. In this case, B is simplified into

$$B = 2(9+4c_0^2 l_p^2)(1+c_0^2 l_p^2)\{L - 3l_p + 4Lc_0^2 l_p^2 + 4c_0^2 l_p^3 - l_p(1+4c_0^2 l_p^2)e^{-L/l_p} + 4l_p e^{-L/2l_p}[\cos(c_0 L) - 2c_0 l_p \sin(c_0 L)]\}. \tag{51}$$

For a very long filament $L \gg l_p$, we get

$$\mathcal{X} = \frac{2 f l_p L}{1+4c_0^2 l_p^2}. \tag{52}$$

As expected, increasing c_0 leads to a smaller $\mathcal{X}$. It also suggests that in this case we can replace l_p in WLC model by $l_p^{\mathrm{eff}\ 1}$ to get correct results. However, similar to the case for R^2 at $f=0$, we should remind that such a replacement is appropriate only if L is rather long or c_0 is small. For large c_0, considerable discrepancies can last up to moderate L (in general $<10 l_p$) though the discrepancy decay faster with increasing L than that on R^2, due to the existence of the term with e^{-L/l_p} in B.

Let us now consider the limit of large stretching force. In this case the filament is almost straight, hence $|\phi| \ll 1$ and $\cos\phi \approx 1-\frac{1}{2}\phi^2$. This transforms Eq. (39) into a form that is equivalent to the Schrödinger equation for a one-dimensional simple harmonic oscillator with mass$=l_p$, $\hbar=1$ and angular frequency $\omega=\sqrt{f/l_p}$

$$\frac{1}{2l_p}\frac{d^2 G_n}{d\phi^2} - \frac{1}{2} f \phi^2 G_n = -\left(g_n + f - \frac{1}{2}c_0^2 l_p\right) G_n. \tag{53}$$

The eigenfunction G_n can be written

$$G_n(\phi) = A_n e^{-(1/2)\xi^2 \phi^2} H_n(\xi\phi), \tag{54}$$

where n is a non-negative integer, $A_n=\sqrt{\xi/(2^n\sqrt{\pi}n!)}$ is the normalization constant, $\xi=\sqrt{l_p \omega}$, and $H_n(x)$ is the Hermite polynomial. The eigenvalues are

$$g_n = \left(n+\frac{1}{2}\right)\sqrt{\frac{f}{l_p}} - f + \frac{1}{2}c_0^2 l_p. \tag{55}$$

Therefore, the partition function can be written as

$$\mathcal{Z}(\phi_L,\phi_0;L,0)=\sum_{n=0}^{\infty} G_n(\phi_0)G_n(\phi_L)e^{-g_nL+c_0l_p(\phi_0+\phi_L)}. \tag{56}$$

Under the limit of large L, we only need to take the first term in the sum [4]. Integrating over all possible values of ϕ_0 and ϕ_L, we get $\mathcal{Z}(L)\sim e^{-g_0L}$. Substituting this result into Eq. (34) leads immediately to

$$\frac{\langle x_L\rangle}{L}=1-\frac{1}{4\sqrt{fl_p}}. \tag{57}$$

It is exactly the same as that for WLC model [24,41]. Under this limit, the extension is independent of c_0, similar to Marko and Siggia's argument that under a strong stretching force, the disorder is immaterial [4]. But the expression is different from its three-dimensional counterpart [4].

V. CONCLUSION AND DISCUSSION

In summary, we find exact expressions for the azimuth angle of a two-dimensional filament in different conditions and at zero temperature. These expressions are sensitive to direction of applied force and boundary conditions. Especially, we find that for a long filament with $\phi_0>0$ and under large stretching force, $\phi(s)$ must be a two-valued function of s, decreases down to a minimum value first, and then increases with increasing s. Otherwise, $\phi(s)$ is always a monotonic function of s. Such a sensitivity of the expressions for $\phi(s)$ to the direction of applied force and ϕ_0 may also be instructive for the relevant three dimensional problems. In special, if we cannot fix the initial orientation angle, at zero temperature a three-dimensional filament under uniaxial external force should have the same shape as given in Eq. (20), since the system has a rotational symmetry with respect to x axis. Similarly, results on the case with fixed ϕ_0 should also be valid, even in three-dimensional systems, if $\mathbf{t}_0$ and f_x happen to be coplanar with the spontaneous curvature. At finite temperature, we obtain exact results for the partition function and end-to-end distance for the filament free of external force. We find that if a filament is very long or c_0 is small, the effect of c_0 can be replaced by a simple correction to the persistence length in the WLC model. However, up to a moderate length and not too small c_0, such a correction becomes poor or even invalid. We obtain closed-form expression for the relationship between force and extension for a filament under low force, and for a long filament under strong stretching force. We find that at low force, up to a moderate length and a not too small c_0, the elasticity of the filament cannot be described by the WLC model, even with a renormalization of the persistence length. However, for a long filament under strong force, c_0 play no role and, therefore, the WLC model can be applied directly to account for the elasticity of the filament. Our results suggest that for short DNA with special sequence order or moderate length DNA with LRC, their mechanical properties may be quite different from the existing results. We do not consider a looped shape at zero temperature in this work. A looped filament may be formed if the filament is rather long ($L>2\pi/c_0$), but in this case the entropic effect should be non-negligible. Another possibility to form a looped filament involves in different boundary conditions, i.e., one has to fix the distance between two ends instead of applying an external force at one end. Finally, in this work, we do not consider the excluded volume effect. This effect is negligible for a short filament at low temperature, but may become rather important for a long filament at finite temperature or for a looped filament. Therefore, the investigation on this effect together with the elastic response to the moderate force at finite temperature should be an intriguing topic of future research.

ACKNOWLEDGMENTS

This work has been supported by the National Science Council of the Republic of China under Grant No. NSC 95-2112-M-032-007, and Physics Division, National Center for Theoretical Sciences at Taipei, National Taiwan University, Taiwan, ROC.

APPENDIX A

1. SOME BASIC PROPERTIES FOR ELLIPTIC INTEGRALS AND ELLIPTIC FUNCTIONS

For convenience, we present here the definitions and some basic properties for $F(\theta|k)$, $\mathrm{am}(x|k)$, and $\mathrm{sn}(x|k)$ used in this work [38–40].

The elliptic integral of the first kind is defined by

$$F(\theta|k)\equiv\int_0^{\theta}\frac{dx}{\sqrt{1-k^2\sin^2x}}. \tag{A1}$$

The Jacobi amplitude function $\mathrm{am}(x|k)$ is the inverse function of $F(\theta|k)$, and the Jacobi elliptic function $\mathrm{sn}(x|k)$ is defined by $\mathrm{sn}(x|k)\equiv\sin[\mathrm{am}(x|k)]$. The complete elliptic integral of the first kind is defined by $K(k)\equiv F(\pi/2|k)$. $\mathrm{sn}(x|k)$ satisfies $\mathrm{sn}[x+2K(k)|k]=-\mathrm{sn}(x|k)$, and so does for $\mathrm{am}(x|k)$. $\mathrm{am}(x|k)$ is also an odd function of x, i.e., $\mathrm{am}(x|k)=-\mathrm{am}(-x|k)$.

Furthermore, though the right-hand side in Eq. (A1) is well defined even for $k>1$, most of the well known properties for elliptic integrals and elliptic functions are based on $k<1$. Therefore, in the case of $k>1$, it would be better to let $k_1=1/k$, $\sin y=k\sin x$, so $dx=k_1\cos y dy/\cos x$, $\cos y=\sqrt{1-k^2\sin^2x}$, $\cos x=\sqrt{1-k_1^2\sin^2y}$, and

$$\int_0^{\theta}\frac{dx}{\sqrt{1-k^2\sin^2x}}=k_1\int_0^{\zeta}\frac{dy}{\sqrt{1-k_1^2\sin^2y}}=k_1F(\zeta|k_1), \tag{A2}$$

where $\zeta=\arcsin(k\sin\theta)$.

2. ON THE BOUND OF INTEGRATIONS

In Sec. III, the main topic is to deal with the integration in the form of

$$J \equiv \int_{\theta_0}^{\theta} \frac{dx}{\sqrt{A-\cos x}}. \tag{A3}$$

Here we show that J is, in general, bounded except for $A \to 1$ and $\theta_0 \to 0$.

If $\pi/2 > \theta > \theta_0$ and $A > 0$, then

$$\int_{\theta_0}^{\theta} \frac{dx}{\sqrt{A-\cos x}} < \frac{\theta-\theta_0}{\sqrt{A-\cos\theta_0}}. \tag{A4}$$

Therefore, if $A > \cos\theta_0$ and θ is bounded, then J is also bounded. Even if $A = \cos\theta_0$ but $A \neq 1$, J is still bounded. This is because around θ_0, we have

$$\int_{\theta_0}^{\theta_0+\varepsilon} \frac{dx}{\sqrt{\cos\theta_0-\cos x}} \sim \int_{\theta_0}^{\theta_0+\varepsilon} \frac{dx}{\sqrt{\sin\theta_0(x-\theta_0)}} = \frac{2\sqrt{\varepsilon}}{\sin\theta_0}, \tag{A5}$$

where ε is a small number. J is unbounded only when $A \sim 1$ and $\theta_0 \sim 0$, because in this case

$$\begin{aligned}\int_{\theta_0}^{\theta_0+\varepsilon} \frac{dx}{\sqrt{A-\cos x}} &\sim \int_0^{\varepsilon} \frac{dx}{\sqrt{1-\cos x}} \\ &= \int_0^{\varepsilon} \frac{dx}{\sqrt{2\sin^2(x/2)}} \\ &\sim \sqrt{2}\int_0^{\varepsilon} \frac{dx}{x} \to \infty .\end{aligned} \tag{A6}$$

3. DERIVATION OF EQS. (14) and (15)

If $c_0 = 0$ and $F_x > 0$, let $k_0 \equiv \cos(\phi_L/2)$ and $\cos(x/2) = k_0 \sin y$, we have $dx = -2k_0 \cos y dy/\sin(x/2)$ and $\sin(x/2) = \sqrt{1-k_0^2\sin^2 y}$. From Eq. (10) we find

$$\begin{aligned}s &= -\int_{\phi_0}^{\phi} \frac{dx}{\sqrt{F_x(\cos\phi_L-\cos x)}} \\ &= -\frac{1}{\sqrt{2F_x}}\int_{\phi_0}^{\phi} \frac{dx}{\sqrt{k_0^2-\cos^2(x/2)}} \\ &= \sqrt{\frac{2}{F_x}}\int_{\theta_0}^{\theta} \frac{dy}{\sqrt{1-k_0^2\sin^2 y}} \\ &= \sqrt{\frac{2}{F_x}}[F(\theta|k_0)-F(\theta_0|k_0)],\end{aligned} \tag{A7}$$

where $\theta = \arcsin[\cos(\phi/2)/k_0]$.

If $c_0 = 0$ and $F_x < 0$, let $k_0' = \sin(\phi_L/2)$, from Eqs. (7) and (A2) we find

$$\begin{aligned}s &= \frac{1}{\sqrt{-2F_x}k_0'}\int_{\phi_0}^{\phi} \frac{dx}{\sqrt{1-\frac{1}{k_0'^2}\sin^2(x/2)}} \\ &= \frac{2}{\sqrt{-2F_x}k_0'}\int_{\phi_0/2}^{\phi/2} \frac{dy}{\sqrt{1-\frac{1}{k_0'^2}\sin^2 y}} \\ &= \sqrt{\frac{-2}{F_x}}[F(\beta|k_0')-F(\beta_0|k_0')],\end{aligned} \tag{A8}$$

where $\beta = \arcsin[\sin(\phi/2)/k_0']$. Equations (A7) and (A8) lead to Eqs. (14) and (15).

4. DERIVATION OF EQ. (20)

When $c_0 \neq 0$ and $F_x > 0$, let $k^2 \equiv \frac{1}{2}(1 + c_0^2/F_x + \cos\phi_L)$ and $x/2 = \pi/2 - y$, from Eq. (17) we obtain

$$\begin{aligned}s &= \frac{1}{\sqrt{2F_x}}\int_{\phi_0}^{\phi} \frac{dx}{\sqrt{k^2-\cos^2(x/2)}} \\ &= -\sqrt{\frac{2}{F_x}}\int_{\alpha_0}^{\alpha} \frac{dy}{\sqrt{k^2-\sin^2 y}} \\ &= -\sqrt{\frac{2}{F_x}}k_1[F(\alpha|k_1)-F(\alpha_0|k_1)],\end{aligned} \tag{A9}$$

where $\alpha = \pi/2 - \phi/2$, $\alpha_0 = \pi/2 - \phi_0/2$, and $k_1 = 1/k \leq 1$. Therefore,

$$\phi(s) = \pi - 2\,\mathrm{am}\left(-\sqrt{\frac{F_x}{2}}ks + F(\alpha_0|k_1)|k_1\right). \tag{A10}$$

It is just Eq. (20). From Eqs. (18) and (A9), we obtain

$$\frac{L}{2} = -\sqrt{\frac{2}{F_x}}k_1[K(k_1)-F(\alpha_0|k_1)] \tag{A11}$$

or

$$-kL\sqrt{\frac{F_x}{2}} + F(\alpha_0|k_1) = 2K(k_1) - F(\alpha_0|k_1). \tag{A12}$$

So

$$\begin{aligned}&\mathrm{am}\left(-\sqrt{\frac{F_x}{2}}k(L-s) + F(\alpha_0|k_1)|k_1\right) \\ &= \mathrm{am}\left(\sqrt{\frac{F_x}{2}}ks - F(\alpha_0|k_1) + 2K(k_1)|k_1\right) \\ &= -\mathrm{am}\left(\sqrt{\frac{F_x}{2}}ks - F(\alpha_0|k_1)|k_1\right) \\ &= \mathrm{am}\left(-\sqrt{\frac{F_x}{2}}ks + F(\alpha_0|k_1)|k_1\right),\end{aligned} \tag{A13}$$

where we have used the properties that $\mathrm{am}(x+2K(k)|k) = -\mathrm{am}(x|k)$, and $\mathrm{am}(x|k) = -am(-x|k)$. That means Eq. (20) is symmetric with respect to the interchange of s and $L-s$.

APPENDIX B: DERIVATION OF B IN EQ. (50)

For the filament free of force, from Eq. (43), we can find that

$$\langle x_L\rangle = \int_0^L ds \int_0^{2\pi} d\phi \cos\phi Z(\phi,s;\phi_0,s_0=0)$$

$$= \frac{2l_p}{1+4c_0^2l_p^2}\{\cos\phi_0 - 2c_0l_p\sin(\phi_0) - e^{-L/2l_p}[\cos(\phi_0+c_0L) - 2c_0l_p\sin(\phi_0+c_0L)]\}, \tag{B1}$$

$$\langle x_L^2\rangle = 2\int_0^L ds\int_0^s ds'\int_0^{2\pi} d\phi\int_0^{2\pi} d\phi' Z(\phi,s;\phi',s')\cos\phi\cos\phi' Z(\phi',s';\phi_0,s_0=0)$$

$$= 2\int_0^L ds\int_0^s ds'\int_0^{2\pi} d\phi' \cos[\phi'+c_0(s-s')]\cos\phi' Z(\phi',s';\phi_0,s_0=0)e^{-(s-s')/2l_p}$$

$$= 2\int_0^L ds\int_0^s ds'\int_0^{2\pi} d\phi' \cos[\phi'+c_0(s-s')]\cos\phi' e^{-(s-s')/2l_p}\left(\frac{1}{2\pi}+\frac{1}{\pi}e^{-(2/l_p)s'}\cos[2(\phi'-\phi_0)-2c_0s']\right)$$

$$= \int_0^L ds\int_0^s ds'\{e^{-(s-s')/2l_p}\cos[c_0(s-s')] + e^{-(s+3s')/2l_p}\cos[c_0(s+s')+2\phi_0]\}. \tag{B2}$$

The final expression of $\langle x_L^2\rangle$ is lengthy, but less useful, so we do not present it here. Instead, we obtain

$$\langle x_L^2\rangle - \langle x_L\rangle^2 = \frac{l_pB}{(1+4c_0^2l_p^2)^2(9+4c_0^2l_p^2)(1+c_0^2l_p^2)}, \tag{B3}$$

$$B \equiv (9+4c_0^2l_p^2)\left\{(8c_0^2l_p^2-1)l_p\cos(2\phi_0) + 2\left[(c_0^2l_p^2+1)(L-3l_p+4Lc_0^2l_p^2+4c_0^2l_p^3) + c_0l_p^2\left(\frac{5}{2}-2c_0^2l_p^2\right)\sin(2\phi_0)\right]\right\}$$
$$- l_p(1+4c_0^2l_p^2)^2e^{-2L/l_p}\{(2c_0^2l_p^2-3)\cos[2(c_0L+\phi_0)] + 5c_0l_p\sin[2(c_0L+\phi_0)]\}$$
$$- 4l_p(9+13c_0^2l_p^2+4c_0^4l_p^4)e^{-L/l_p}[\cos(c_0L+\phi_0) - 2c_0l_p\sin(c_0L+\phi_0)]^2$$
$$+ 8l_p(c_0^2l_p^2+1)e^{-L/2l_p}\{(9+4c_0^2l_p^2)\cos(c_0L) + (3-20c_0^2l_p^2)\cos(c_0L+2\phi_0)$$
$$- 2c_0l_p[(9+4c_0^2l_p^2)\sin(c_0L) + (7-4c_0^2l_p^2)\sin(c_0L+2\phi_0)]\}. \tag{B4}$$

When $T\to 0$, we obtain $\langle x_L^2\rangle = \langle x_L\rangle^2 = 4\sin^2(c_0L/2)\cos^2(c_0L/2+\phi_0)/c_0^2$ as it should be for the x component of the end-to-end distance of an arc with radius $1/c_0$.

[1] O. Kratky and G. Porod, Recl. Trav. Chim. Pays-Bas **68**, 1106 (1949).
[2] J. F. Marko and E. D. Siggia, Science **265**, 506 (1994).
[3] C. Bustamante, J. F. Marko, E. D. Siggia, and S. Smith, Science **265**, 1599 (1994).
[4] J. F. Marko and E. D. Siggia, Macromolecules **28**, 8759 (1995).
[5] S. B. Smith, L. Finzi, and C. Bustamante, Science **258**, 1122 (1992).
[6] T. R. Strick, J. F. Allemand, D. Bensimon, A. Bensimon, and V. Croquette, Science **271**, 1835 (1996).
[7] P. Cluzel, A. Lebrun, C. Heller, R. Lavery, J. L. Viovy, D. Chatenay, and F. Caron, Science **271**, 792 (1996).
[8] S. B. Smith, Y. Cui, and C. Bustamante, Science **271**, 795 (1996).
[9] B. Fain, J. Rudnick, and S. Östlund, Phys. Rev. E **55**, 7364 (1997).
[10] J. F. Marko, Phys. Rev. E **55**, 1758 (1997).
[11] J. D. Moroz and P. Nelson, Proc. Natl. Acad. Sci. U.S.A. **94**, 14418 (1997).
[12] A. Goriely and M. Tabor, Proc. R. Soc. London, Ser. A **453**, 2583 (1997).
[13] H. Zhou and Z.-C. Ou-Yang, J. Chem. Phys. **110**, 1247 (1999).
[14] H. Zhou, Y. Zhang, and Z.-C. Ou-Yang, Phys. Rev. E **62**, 1045 (2000).
[15] S. V. Panyukov and Y. Rabin, Phys. Rev. E **64**, 011909 (2001).
[16] D. A. Kessler and Y. Rabin, Phys. Rev. Lett. **90**, 024301 (2003).
[17] Z. Zhou, P.-Y. Lai, and B. Joós, Phys. Rev. E **71**, 052801 (2005).
[18] E. N. Trifonov, R. K.-Z. Tan, and S. C. Harvey, in *DNA Bending and Curvature*, edited by W. K. Olson, M. H. Sarma, and

M. Sundaralingam (Adenine Press, Schenectady, 1987).
[19] P. C. Nelson, Phys. Rev. Lett. **80**, 5810 (1998).
[20] D. Bensimon, D. Dohmi, and M. Mezard, Europhys. Lett. **42**, 97 (1998).
[21] Y. O. Popov and A. V. Tkachenko, Phys. Rev. E **76**, 021901 (2007).
[22] S. Rappaport and Y. Rabin, Macromolecules **37**, 7847 (2004).
[23] J. Moukhtar, E. Fontaine, C. Faivre-Moskalenko, and A. Arneodo, Phys. Rev. Lett. **98**, 178101 (2007).
[24] A. Prasad, Y. Hori, and J. Kondev, Phys. Rev. E **72**, 041918 (2005).
[25] D. Chaudhuri, Phys. Rev. E **75**, 021803 (2007).
[26] R. Brak, A. J. Guttmann, and S. G. Whittington, J. Phys. A **25**, 2437 (1992).
[27] G. Fleer, M. C. Stuart, J. Scheutjens, T. Cosgrove, and B. Vincent, *Polymers at Interfaces* (Chapman and Hall, London, 1993).
[28] S. C. Bae, F. Xie, S. Jeon, and S. Granick, Curr. Opin. Solid State Mater. Sci. **5**, 327 (2001).
[29] D. Marenduzzo, A. Maritan, A. Rosa, and F. Seno, Phys. Rev. Lett. **90**, 088301 (2003).
[30] A. Rosa, D. Marenduzzo, A. Maritan, and F. Seno, Phys. Rev. E **67**, 041802 (2003).
[31] H. Zhou, J. Zhou, Z.-C. Ou-Yang, and S. Kumar, Phys. Rev. Lett. **97**, 158302 (2006).
[32] W. Han, S. M. Lindsay, M. Dlakic, and R. E. Harrington, Nature (London) **386**, 563 (1997).
[33] W. Han, M. Dlakic, Y.-J. Zhu, S. M. Lindsay, and R. E. Harrington, Proc. Natl. Acad. Sci. U.S.A. **94**, 10565 (1997).
[34] H. R. Drew and A. A. Travers, J. Mol. Biol. **186**, 773 (1985).
[35] M. Dlakic, K. Park, J. D. Griffith, S. C. Harvey, and R. E. Harrington, J. Biol. Chem. **271**, 17911 (1996).
[36] H. Kleinert, *Path Integrals in Quantum Mechanics, Statistics, and Polymer Physics* (World Scientific, Singapore, 1990).
[37] N. W. McLachlan, *Theory and Application of Mathieu Functions* (Clarendon Press, Oxford, 1947).
[38] S. Wolfram, *The Mathematica Book*, 5th ed. (Wolfram MediaInc., Champaign, 2003).
[39] P. F. Byrd, *Handbook of Elliptic Integrals for Engineers and Scientists*, 2nd ed. (Springer-Verlag, Berlin, 1971).
[40] S. Lang, *Elliptic Functions* (Addison-Wesley, Advanced Book Program, Reading, MA, 1973).
[41] I. M. Kulić, H. Mohrbach, R. Thaokar, and H. Schiessel, Phys. Rev. E **75**, 011913 (2007).